Research Square

Preprints are preliminary reports that have not undergone peer review.
They should not be considered conclusive, used to inform clinical practice,
or referenced by the media as validated information.

Holistic compression model to predict post-stroke mood at 6 months

Suhrit Duttagupta

suhrit.duttagupta@u-bordeaux.fr

University of Bordeaux

Michel Thiebaut de Schotten

Neurodegeneratives Diseases Institute

Thomas Tourdias

University of Bordeaux

Olivier Godefroy

Centre Hospitalier Universitaire Amiens-Picardie

Sylvie Berthoz

University of Bordeaux

Igor Sibon

University of Bordeaux

Research Article

Keywords: Stroke, Neuroimaging, Predictive model, Post-stroke depression, Post-stroke anxiety, Whole-brain

Posted Date: April 17th, 2026

DOI: https://doi.org/10.21203/rs.3.rs-9313883/v1

License: This work is licensed under a Creative Commons Attribution 4.0 International License.
Read Full License

Additional Declarations: No competing interests reported.

Holistic compression model to predict post-stroke mood at 6 months

Suhrit Duttagupta[a], Michel Thiebaut de Schotten[b,c], Thomas Tourdias[d,e], Olivier Godefroy[f,g]

Sylvie Berthoz[a,h], Igor Sibon[a,i]

[a]Univ. Bordeaux, INCIA UMR 5287, Bordeaux, France 33000.

[b]Groupe d'Imagerie Neurofonctionnelle, Institut des Maladies Neurodégénératives 5293, Centre National de la Recherche Scientifique, Bordeaux, France 33000

[c]Brain Connectivity and Behaviour Laboratory, Sorbonne University, Paris, France 75013

[d]Univ. Bordeaux, Neurocentre Magendie UMR 1215, Bordeaux, France 33000

[e]CHU Bordeaux, Diagnostic and Therapeutic Neuroimaging Unit, Bordeaux, France 33000

[f]Department of Neurology, Amiens University Hospital, Amiens, France 80000

[g]Laboratory of Functional Neurosciences (Research Unit 4559), Jules Verne University of Picardie, Amiens, France 80000

[h]Department of Psychiatry for Adolescents and Young Adults, Institut Médico-chirurgical Montsouris, Paris, France 75014

[i]CHU Bordeaux, Stroke Unit, Bordeaux, France 33000

ORCID ID (Email):

Suhrit Duttagupta: 0000-0002-1592-9301 (Corresponding author: suhrit.duttagupta@u-bordeaux.fr)

Michel Thiebaut de Schotten: 0000-0002-0329-1814

Thomas Tourdias: 0000-0002-7151-6325

Olivier Godefroy: 0000-0001-6789-6620

Sylvie Berthoz: 0000-0002-6862-2362

Igor Sibon: 0000-0002-1171-4215

ACKNOWLEDGEMENTS

The authors would like to thank Stéphane Olindo, Pauline Renou, Sabrina Debruxelles, Mathilde Poli, Sharmila Sagnier and Pierre Briau from the Stroke Unit of the Bordeaux University Hospital, who were instrumental in patient recruitment in the BBS and MOTIV-POSDEP cohorts. We are also grateful to the Clinical Epidemiology Unit (USMR) for providing data for the cohorts.

ABSTRACT

Introduction: Mood impairments are frequent after stroke yet remain difficult to predict using neuroimaging markers. While voxel-level analyses have struggled to identify reliable predictors, network-level approaches may offer improved sensitivity. Accordingly, we developed a pipeline to predict post-stroke mood status using whole-brain components derived from MRI sequences routinely acquired in clinical practice.

Methods: Three heterogeneous stroke cohorts (n_{total} = 672) were included, with mood evaluated six months post-stroke using the Hospital Anxiety and Depression (HAD) and Center for Epidemiologic Studies–Depression (CES-D) scales. For model training, diffusion-weighted signal from one cohort was compressed using principal component analysis (PCA), and components associated with mood scores were used in nonparametric regression models. Predictive performance was externally validated and compared with disconnectome-based models and models based on baseline clinical and demographic variables. Disconnectome-based models showed minimal predictive power across datasets (R^2 < 0.01). The imaging-based pipeline modestly outperformed clinical models for predicting CES-D scores (ΔAUC = 0.046, $p < 0.001$; $\Delta R^2 = 0.056$), in the absence of baseline mood measures. For HAD outcomes, clinical models performed best for anxiety (AUC = 0.735) and depression (AUC = 0.795), with baseline mood status as the strongest predictor. The proposed pipeline achieved moderate predictive performance for HAD anxiety (AUC = 0.613) and depression (AUC = 0.708).

Conclusion: Overall, predictive performance remained limited across all approaches, highlighting the heterogeneity in neuropsychiatric predictions. This novel framework to capture global diffusion patterns without requiring advanced imaging sequences may provide complementary information for identifying neural components associated with neuropsychiatric dysfunction.

Keywords: Stroke, Neuroimaging, Predictive model, Post-stroke depression, Post-stroke anxiety, Whole-brain

INTRODUCTION

Understanding how brain structure gives rise to behavior remains challenging due to the immense number of factors influencing mental functioning. Early neuroscientific work adopted a reductionist framework, assuming that behaviors or symptoms could be traced to discrete brain regions in isolation (Bickle, 2012; Parker, 2023). However, accumulating evidence shows that this assumption breaks down for higher-order cognition. Contemporary research increasingly emphasizes holistic descriptions of cerebral activity.

The limitations of reductionism are well illustrated in studies linking stroke lesions to neuropsychological outcomes. Non-motor impairments - particularly socioaffective disturbances - rarely depend on the infarct location alone, but arising from interactions among distributed brain regions instead (Herbet & Duffau, 2020). Prognosis in the chronic post-stroke stage cannot be reliably inferred from lesion location without considering clinical and demographic factors such as sex or medical history. This reflects the fact that brain regions operate within functional circuits rather than as isolated modules (Parker & Friston, 2013; Bota et al., 2015). For example, damage to Broca's area may impair language, but lesions affecting the white-matter tracts connecting frontal, parietal, and temporal regions can produce similar deficits (Thiebaut de Schotten et al., 2015). Consequently, white-matter disconnectivity, or the "disconnectome", has been proposed as a more accurate neuroimaging predictor of post-stroke outcomes (Lim et al., 2021; Thiebaut de Schotten & Forkel, 2022).

Building on this idea, Talozzi et al. (2023) introduced the Disconnectome Symptom Discoverer (DSD), an online tool that predicts long-term motor, functional, and cognitive outcomes from three-dimensional lesion images. The tool estimates each patient's disconnectome based on the degree to which their infarct disrupts surrounding white-matter tracts. These disconnectomes are then compressed using uniform manifold approximation and projection (UMAP), which reduces high-dimensional data into a low-dimensional representation (Lovrić et al., 2021). Each patient is represented as a point in a shared "morphospace," which is subsequently linked to clinical scores to build predictive models. This approach offers a middle ground: it is broader in scope than voxel-based lesion analyses yet more feasible for clinical use than whole-brain diffusion-tensor connectomics. Nonetheless, methodological concerns remain. First, the UMAP dimensions are determined by the training dataset and are therefore arbitrary; the distribution of lesions in the training cohort shapes the entire morphospace, potentially biasing representation of under- or over-sampled regions. Second, the DSD relies on parametric statistics, despite clinical data often being non-parametric, which may obscure non-linear relationships between disconnectivity and symptoms (Bolboacă, 2019).

Importantly, the DSD was not trained to predict post-stroke mood impairments. Conditions such as post-stroke depression (PSD) and post-stroke anxiety (PSA) affect roughly one-third of patients each, yet remain undertreated, partly due to difficulties in predicting their onset and trajectory (Medeiros et al., 2020; Ferro et al., 2016). Even beyond the context of stroke, the link between neuroanatomy and mood disorders is weak; despite extensive research, affective dysfunction cannot be localized beyond the level of distributed neural circuits (Pessoa et al., 2023; Oakes et al., 2017). No lesion location or structural feature has been consistently associated with PSD, and the literature on PSA is even more limited (Robinson et al., 2024; Moore et al., 2024). This challenge was highlighted in the recent NEURAL Cup competition, which evaluated models predicting long-term post-stroke symptoms from acute imaging: despite diverse approaches, including disconnectivity, parcellation, and neural networks, PSA and PSD predictions showed the lowest performance among neuropsychological outcomes (Matsulevits et al., 2025). These findings underscore the need for neuroimaging markers that capture broad, distributed patterns of brain organization rather than relying on fine-grained voxel-level analyses.

In this study, we introduce a methodological pipeline for predicting post-stroke mood impairments using linear compression of routine clinical MRI scans. Although the pipeline can incorporate any imaging sequence, we used diffusion-weighted images to approximate diffusion-tensor information. Our objectives were to: (1) extract whole-brain diffusivity patterns using principal component analysis across a complete MRI cohort; (2) identify components significantly associated with post-stroke anxiety and depression symptomatology; and (3) compare the predictive performance of this model with clinical and disconnectome-based models in independent cohorts.

MATERIALS AND METHODS

DATA COLLECTION

Clinical diffusion-weighted imaging (DWI) scans taken at patient admission were obtained from three French stroke cohorts:

1. Brain Before Stroke (BBS): conducted between June 2012 and February 2015 (French Research ID: PHRC-12-152) (Munsch et al., 2016). Primary inclusion criteria were: adults with a clinical diagnosis of minor-to-severe supratentorial ischemic stroke (National Institutes of Health Stroke Scale (NIHSS) between 1 and 25) between 24 and 72 hours after the onset. Exclusion criteria were history of symptomatic ischemic stroke with functional deficit

(prestroke modified Rankin Scale [mRS] score ≥1), infratentorial stroke, history of dementia or psychosis. DWI scans were obtained using a General Electric 3T scanner with TE 82 ms, TR 9000 ms, voxel size 0.94 x 0.94 x 4.5 mm^3, field of view 24 x 24 cm^2, slice thickness 4 mm, and slice gap 0.5 mm.

2. Groupe de Réflexion pour l'Évaluation Cognitive Vasculaire (GRECOGVasc, ClinicalTrials: NCT01339195): conducted between September 2010 and November 2016 (Godefroy et al., 2012). For the present analyses, a subgroup of the cohort was taken, for which the inclusion criteria were consenting French-speaking patients between ages 40 and 80, hospitalized for cerebral infarct within the past 30 days with initial positive DWI imaging, a reliable informant, and no previously diagnosed conditions - other than a previous stroke - affecting cognition. DWI scans were obtained using a General Electric SIGNA Prime 1.5T scanner with TE 97.6 ms, TR 9650 ms, voxel size 1.02 x 1.02 x 6 mm^3, field of view 12 x 12 cm^2, slice thickness 4 mm, and slice gap 4 mm.

3. MObile Technologies In the preVention of POSt-stroke DEPression (MOTIV-POSDEP, ClinicalTrials: NCT04043052) cohort: conducted between September 2020 and September 2023 (Duttagupta et al., 2026). Primary inclusion criteria were: first-ever stroke within the past 15 days and no severe handicap (mRS score above 3) or cognitive impairment (Montreal Cognitive Assessment [MoCA] score under 16). The primary exclusion criteria were post-stroke severe aphasia (NIHSS item 9 ≥ 2), current or recent (within the 6 months preceding stroke) anxiety or depressive disorder as assessed by the Mini International Neuropsychiatric Interview version DSM 5, or psychoactive drug use. DWI images were obtained using a SIEMENS Magnetom Altea 1.5 T scanner with TE 78 ms, TR 5000 ms, voxel size 0.78 x 0.78 x 2.4 mm^3, field of view 27.0 x 24.5 cm^2, slice thickness 2 mm and slice gap 2.4 mm.

The following demographic and clinical baseline data were collected: age, sex, pre-stroke functional and cognitive status (measured using the modified Rankin Scale and the Informant Questionnaire on Cognitive Decline in the Elderly, respectively), the NIHSS score at admission, and the cognitive status during hospital stay (assessed using the Montreal Cognitive Assessment). Stroke lesion volume was considered as a clinical variable for the purpose of analysis, computed from binarized lesion masks. Kruskal-Wallis and χ^2 tests were used to evaluate the heterogeneity of the cohorts.

The mood variables were scores from (i) the Hospital Anxiety and Depression (HAD) scale, with a range of possible scores for both the Anxiety and Depression subscales between 0 and 21 (Lépine et al., 1985), and (ii) the Center of Epidemiological Studies-Depression Scale (CES-D) (Morin et al., 2011), with a range of possible scores between 0 and 60. The anxiety

and depression subscales from the HAD have a clinical threshold score of 8 or above, while the most commonly used clinical threshold for depression using the CES-D is a score of 16 or above.The HAD was administered in the BBS and MOTIV-POSDEP cohorts at baseline and the 6-month follow-up, while the CES-D was administered in GRECOGVasc and MOTIV-POSDEP only at the 6-month follow-up.

IMAGE PROCESSING

The DWI sequences in all cohorts were encoded within three-directions and had b-values of 0 and 1000 s/mm^2. Mean diffusion-weighted images were computed (isotropic images) and skull-stripped using the HD-BET tool (Isensee et al., 2019). The images were normalized using the non-linear transformation of Advanced Normalization Tools in Python (ANTSpy) (Avants et al., 2009), using a DWI MNI 1mm template derived from the Human Connectome Project (Van Essen et al., 2012). We used smoothing with a median filter of 3 mm for the BBS cohort to mitigate some unusually high inhomogeneity within the scanner that directly provided mean DWI images.

To confirm the reliability of the pipeline, apparent diffusion coefficient (ADC) maps were generated to be used as an alternative input. ADC represents the magnitude of diffusion that theoretically should remain constant across different MRI machines, but slight variations are produced due to anisotropy bias and vendor-specific algorithms (Malyarenko et al., 2014).

MODEL DESIGN

The code for the model was written in Python. It is available at https://github.com/SuhritD/pca-prediction-pipeline

Three steps were involved in creating the pipeline:

1. Dataset compression: Each subject's image was taken as a 1-D array of the unravelled intensity values, i.e., an array of size 7221032 for an image of 192 x 218 x 192 voxels. The combined matrix of the data was compressed through principal component analysis (PCA) set to create 100 components. In order to ensure reproducibility of the compressed data, full singular value decomposition was implemented.
2. Component selection: For each clinical evaluation, Spearman correlation was done between the 100 PCA components and the patients' 6-month scores. Components with a correlation coefficient over 0.2 were selected for the particular evaluation. If

more than 4 components were selected, backward linear regression was performed to eliminate non-significant components.

3. Training: Nonparametric regression was conducted between the significant components and mood scores. k-nearest neighbors (k-NN) regression is an algorithm that predicts output values based on the values of the closest training data points (Altman et al., 1992). It is one of the simplest forms of machine learning and is well-suited for fitting non-linear relationships. The number of neighbors selected can significantly affect model performance: for instance, using only one neighbor (k=1) will lead to overfitting because the prediction would rely too heavily on a single data point. While the optimal number of neighbors depends on the specific dataset, using five neighbors (k=5) is often considered a reasonable default. In this study, the value of k was chosen between 2 and 30 based on cross-validation of the regression performance. The model was implemented using the KNeighborsRegressor from the sklearn.neighbors package (Pedregosa et al., 2011; Cunningham & Delany, 2021).

The pipeline configuration was done by taking images from two cohorts: the training sample for HAD Anxiety and Depression scores was the BBS cohort and the validation sample was MOTIV-POSDEP. For the CES-D scores, training was done on the MOTIV-POSDEP cohort and validation on the GRECOGVasc cohort. Apart from the previously noted preprocessing steps, while using mean DWI images, a crucial modification of the validation cohort images is the shifting of intensities - based on the mean range and variance of the images in the original cohort, the intensities of the validation sample images were shifted by ordinal rank to match the pattern of the intensity histogram of the training sample. This is an important modification due to the nature of PCA: it relies on correlations between the columns of the data to capture as much of the data's variance. Due to the multitude of factors differing between the MRI images of different cohorts, it is necessary to shift the intensities to obtain satisfactory results. This can be overcome by either training the model using ADC maps or taking a combination of DWI images across cohorts.

The new images were transformed based on the same PCA to obtain the 100 components for the validation samples and the regression parameters obtained for each evaluation were used to predict the new scores. During the processing stages, the emotional scores were standardized to their z-score based on the complete set of values of the evaluation across cohorts to increase the predictions' generalizability. Compared to studies utilizing the HAD and CES-D at 6 months post-stroke, the mean and standard deviation of our pooled scores matched those of the general stroke population (Knapp et al., 2020; Liu et al., 2023; Liu et al., 2024).

To illustrate the biological nature of relevant PCA components, we created diffusivity maps - for each relevant component, a ranked correlation between the transformed component and each voxel of the DWI intensity matrix was performed. The resulting matrix can be represented as a 3D image with the same dimensions as the normalized DWI images. The heatmap of the diffusivity images can illustrate patterns of high or low intensity values across the brain that are associated with a specific clinical evaluation.

PERFORMANCE COMPARISON

For each evaluation, the pipeline was compared with the DSD and a model using only clinical variables. For the clinical models, a generalized linear model was created to choose the best fit from routine evaluations conducted at hospital stay:

1. Age
2. Sex
3. Admission NIHSS
4. Stroke Volume
5. Pre-stroke IQCODE
6. MoCA
7. Baseline mood status (only for cohorts with HAD scores)

mRS scores could not be used due to the low values.
The GRECOGVasc cohort did not assess baseline mood and hence the variable was not considered for predicting CES-D scores. Additionally, the models for predicting HAD Anxiety and Depression were also fitted without this variable to evaluate its impact.

For the DSD model, the code implemented in Talozzi et al. (2023) was used. Briefly, the steps were: (i) converting normalized lesion masks to disconnectomes through a deep learning tool (Matsulevits et al., 2024), (ii) representing lesions on a UMAP plane of dimensions 280 x 240, (iii) selecting clusters of voxels significantly correlated with a specific clinical evaluation, and (iv) linear regression of the first three PCA components of the clusters to predict the clinical score. For validation, the disconnectomes of another cohort were compressed with the same UMAP before applying the same PCA weights and regressors to obtain the predicted scores.

Goodness-of-fit
We used three metrics: the pseudo R-squared (the squared Pearson correlation coefficient between actual and predicted values), the mean squared error (the mean of the squared

difference between predicted and actual values) and the area under the receiver operating characteristics curve (AUC), which characterizes the discriminative power of the predictive model. A model with 0.5 AUC is equivalent to random chance of predicting whether or not a patient has a score above the clinical threshold. Comparing AUC values between models was done through DeLong's test.

RESULTS

Descriptive Statistics

The descriptive statistics for the three cohorts are presented in Table 1 along with the prevalences of clinically-defined mood disorders. Between-cohort comparisons based on the baseline characteristics are provided in Supplementary Material 1 - briefly, the cohorts were significantly different based on all clinical variables ($p<0.001$) except for pre-stroke cognitive status (IQCODE $p = 0.188$), confirming their heterogeneity.

Table 1: Descriptive statistics of clinical and demographic status of all patients.

	BBS (n=207)	GRECOGVasc (n=282)	MOTIV-POSDEP (n=183)
Sex (M/F)	142/65	172/110	130/53
Age	66 (21) 35-90	65 (18) 40-81	58 (21) 21-89
Admission NIHSS	3 (4) 1-21	3 (5) 0-24	2 (3) 0-18
Pre-stroke mRS	0 (0.00) 0-4	0 (0.00) 0-3	0 (0.00) 0-2
Pre-stroke IQCODE	3 (0.00) 2.30 - 3.90	3 (0.063) 1.88-3.56	3.1 (0.10) 1.00-3.80
Admission MOCA	24 (7.00) 1 - 30	24 (6.00) 0-30	26 (3.00) 17-30

Stroke Volume (cm^3)	7.33 (20.09) 0.09-165.67	1.58 (10.12) 0.001-31.91	0.618 (2.134) 0.01-61.06
Baseline HAD-A	6 (6.00) 0-19	Not recorded	6 (4.00) 0-18
Baseline HAD-D	3 (4.00) 0-18	Not recorded	2 (3.00) 0-13
6-month HAD-A	3 (6.00) 0-21	Not recorded	4 (3.50) 0-15
6-month HAD-D	2 (5.00) 0-18	Not recorded	2 (4.50) 0-18
CES-D	Not recorded	10 (14.8) 0-54	6 (8.50) 0-38
Prevalence of clinically-defined mood disorder (%)			
Baseline HAD-A	14.49		10.38
Baseline HAD-D	17.9		12.8
6-month HAD-A	35.1		34.1
6-month HAD-D	19.32		19.67
CES-D		32.66	13.7

The numerical statistics are median (Inter-quartile range) and range unless mentioned otherwise. CES-D: Centre for Epidemiological Studies-Depression scale; IQ-CODE: Informant Questionnaire on Cognitive Decline in the Elderly scale; HAD-A: Hospital Anxiety and Depression Scale-Anxiety; HAD-D: Hospital Anxiety and Depression Scale-Depression; NIHSS: National Institutes of Health Stroke Scale; MoCA: Montreal Cognitive Assessment; mRS: Modified Rankin score

The univariate analyses of the three mood evaluations using baseline clinical variables as

predictors are reported in Supplementary Material 2. Based on the HAD-A scores, follow-up anxiety was strongly positively correlated with baseline anxiety in both BBS and MOTIV-POSDEP ($p<0.001$), negatively correlated with age only in BBS ($\rho= -0.209$, $p=0.003$), and differing by sex only in MOTIV-POSDEP (F > M, $p=0.013$). Based on the HAD-D scores, follow-up depression was strongly positively correlated with baseline depression ($p<0.01$) and significantly differed by sex only in the BBS cohort (F>M; $p=0.028$). Based on the CES-D scores, follow-up depression was negatively correlated with age only in GRECOGVasc ($\rho = -0.227$, $p<0.001$), negatively correlated with initial MoCA scores only in MOTIV-POSDEP ($\rho = -0.153$, $p=0.039$), and significantly differed by sex only in GRECOGVasc (F>M, $p<0.001$).

Clinical Models

The parameter estimates of the models are in the supplementary material (Supplementary Table 3). The prediction performance in the BBS cohort was moderate for 6-month HAD-A ($R^2 = 0.221$, AUC = 0.776) and 6-month HAD-D ($R^2 = 0.202$, AUC = 0.710) scores. The best predictors in both cases were baseline mood status, sex, and age. Using the same predictors with the MOTIV-POSDEP cohort gave similar performance (HAD-A: $R^2 = 0.215$, AUC = 0.735; HAD-D: $R^2 = 0.265$, AUC = 0.735), although age was not a significant covariate for both models and sex was not a significant factor for HAD-D. Without baseline mood status, the performance was poorer for HAD-A (BBS $R^2 = 0.090$, AUC = 0.688; MOTIV-POSDEP $R^2 = 0.027$, AUC = 0.624) as well as HAD-D (BBS $R^2 = 0.053$, AUC = 0.614; MOTIV-POSDEP $R^2 < 0.01$, AUC = 0.538).

For 6-month CES-D scores, baseline depression was not used as a predictor since it was not evaluated in the GRECOGVasc cohort. Using MOTIV-POSDEP data, the best model comprised admission MoCA and stroke volume, although neither covariates were significant and the model had low predictability ($R^2 = 0.0345$, AUC = 0.639). Validating on the GRECOGVasc sample, the performance was poorer ($R^2 <0.01$, AUC = 0.507) with no significant predictors. Upon adding baseline HAD-D scores to the MOTIV-POSDEP model, the performance increased greatly ($R^2 = 0.244$, AUC = 0.781).

Disconnectome Models

The DSD could not be used for certain evaluations due to a low correlation between disconnectome data and the clinical scores: the MOTIV-POSDEP cohort could not be used to predict HAD-A scores and the GRECOGVasc cohort could not be used to predict CES-D scores. For all three clinical scores, the predictive performance was weak (Validation $R^2 <$

0.01) and no stronger than random chance in training or validation samples. The technical failures of the model are explained in the supplementary material (Supplementary Material 4).

Pipeline Models

All three cohorts could be utilized in the pipeline. The transformed data of 100 components from the PCA explained a majority of the MRI data variance in each cohort (BBS: 83.7%; MOTIV-POSDEP: 95.7%; GRECOGVasc: 97.2%). The order of cohorts for training and validation remained the same (as listed in section 2.3).

To represent the derived brain components, a ranked correlation between each voxel of the raw data matrix and a certain component is done: two examples of diffusivity maps have been displayed in Figure 1, with warmer colors indicating higher diffusion signal intensity from the MRI data. The 6th PCA component from the BBS cohort - explaining 4.83% of the data variance - was positively correlated with 6-month HAD-A scores (Figure 1A-D), showing prominently lower intensity along the corpus callosum. The 4th PCA component from the GRECOGVasc cohort - explaining 1.79% of the data variance - negatively correlated with 6-month CES-D scores (Figure 1E-H), with high intensity in the posterior right hemisphere and relatively low intensity in the frontal lobes and the left temporal lobe.

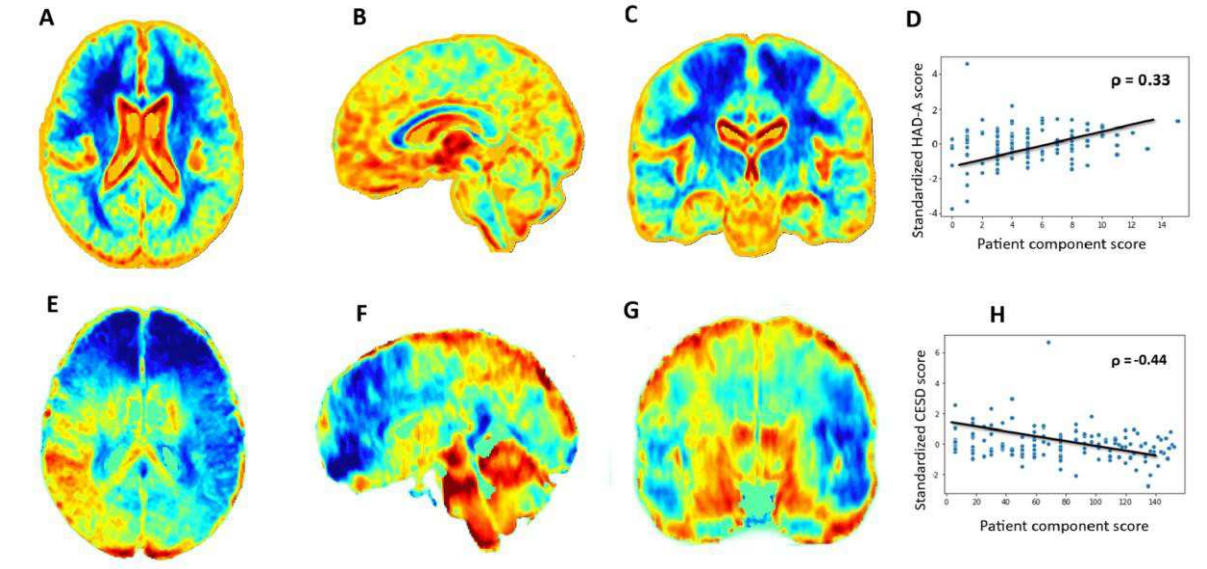


Fig 1. Diffusivity maps associated with mood evaluations (A-C) A component positively correlated with HAD Anxiety and (D-F) a component negatively correlated with the CES-D. The anatomical orientation is inverted. The color map is not to scale. The scatterplots between the transformed

component values and the normalized HAD anxiety (G) and CES-D scores (H) show the corresponding slopes (black) and the Spearman correlation coefficients (ρ).

The pipeline had moderate predictability in the training sample ($R^2 > 0.1$) and was weaker during validation. Compared to the clinical models predicting HAD-A and HAD-D in the validation sample, the capacity to correctly assign clinical mood status was significantly lower (DeLong's test: $p<0.001$). The pipeline model performed better than the clinical model for predicting CES-D scores in the validation sample ($\Delta AUC = 0.046$, $p = 0.01$; $\Delta R^2 = 0.056$) as well as for HAD scores when baseline mood was not included as a covariate.

The performance comparisons of the three models are listed in Table 2. The clinical models showed the best performance except for predicting CES-D scores, while the disconnectome model had the poorest performance in all cases. Additionally, we determined that ADC maps could be used instead of mean DWI images for predicting HAD-A and Depression scores with slightly better performance (Supplementary Material 5).

TABLE 2: Performance comparison between clinical, disconnectome, and whole-brain prediction models.

HAD-A

		Pipeline	Clinical	Disconnectome
Training Sample	**R^2** **MSE** **AUC**	0.11 13.31 0.662	0.16 13.5 0.710	0.025 12.4 0.507
Testing Sample	**R^2** **MSE** **AUC**	0.064 16.03 0.613	0.225 7.13 0.735	0.01 18.6 0.452
HAD-D				
Training Sample	**R^2** **MSE** **AUC**	0.108 10.2 0.721	0.146 11.7 0.765	0.076 21.9 0.618
Testing Sample	**R^2** **MSE** **AUC**	0.067 15.37 0.708	0.268 8.17 0.795	0.004 11.9 0.547
CES-D				
Training Sample	**R^2** **MSE** **AUC**	0.199 72.22 0.718	0.030 17.5 0.630	0.042 18.9 0.522

Testing Sample	**R^2** **MSE** **AUC**	0.078 109.2 0.643	0.022 119.0 0.597	9e-4 132.49 0.421

AUC: Area under the receiver operating characteristic curve; CES-D: Centre for Epidemiological Studies-Depression; HAD: Hospital Anxiety and Depression scale; MSE: Mean squared error; R^2: Coefficient of determination.

DISCUSSION

Based on fundamental principles of data analysis, we designed a model to predict 6-month post-stroke mood scores. With out-of-sample testing from cohorts with heterogeneous populations, our model greatly outperformed a dedicated stroke tool utilizing white matter disconnections.

An important perspective to provide is that, with the exception of initial mood status, no single neuroimaging or clinical variable was a consistently significant predictor across cohorts. Unfortunately, patients are frequently not given mood evaluations during hospital stay, particularly those with low symptom severity. Our findings show that it may be a crucial step for clinicians to develop a long-term prognosis. Although female sex is also considered as a strong predictor of post-stroke mood impairments, it was not significantly associated with follow-up anxiety scores in the BBS cohort, nor was it a significant predictor of follow-up depression scores in the MOTIV-POSDEP cohort. Considering the differences in clinical samples, the moderate but robust performance of our pipeline indicates its validity.

Previous publications on the BBS cohort reported no significant predictors of mood through voxel-based lesion-symptom mapping or diffusion tensor imaging (Sagnier et al., 2019; Sagnier et al., 2020). It is likely that our technique can perform better because instead of relying on fine-grained calculations of specific voxels, we use whole-brain patterns as loose components. The importance of lesion-network analysis in identifying associations with depressive symptoms not available using voxel analysis has been increasingly identified (Ríos et al., 2025; Siddiqi et al., 2023). We implemented a similar data-driven approach to identify gray- and white-matter networks associated with post-stroke fatigue, observing that certain networks were related to specific domains of fatigue (Duttagupta et al., 2026). Furthermore, to the best of our knowledge, this is the first study to evaluate neuroimaging predictors of post-stroke anxiety through network-based analysis. As shown in our data,

anxiety may be more prevalent than depression at the acute or follow-up stages and thus must not be considered as a secondary factor.

The results from the DSD were practically unusable for post-stroke mood status, which is expected due to no robust association between lesion location and mood outcomes being identified in the literature (Robinson et al., 2024; Wei et al., 2015; Medeiros et al., 2020). For models in all cohorts, there were not enough UMAP morphospace voxels correlated with anxiety and depression scores to yield satisfactory results. Unlike PCA, UMAP is a non-linear calculation; its ability to preserve topological structure in the compressed data has been utilized in various domains (Lovrić et al., 2021). Although it would seem that assigning multiple stroke disconnectomes to a compressed plane would yield better results than standard voxel analysis, this was not the case. No significant UMAP voxels were found in the MOTIV-POSDEP cohort with HAD Anxiety scores and the GRECOGVasc cohort with CES-D scores, hence why they could not be used for the training step. Methodologically, certain steps in our pipeline could possibly be implemented in the DSD, such as applying nonparametric statistics and using standardized clinical scores for a better regression fit. However, its critical limitations, i.e., the only input being lesion voxels and the lack of a coherent disconnectome map formed in the UMAP plane, cannot be altered.

The neural architecture of relevant DWI components can be observed by generating diffusivity maps based on the association between the raw and compressed MRI data, as shown in Figure 1. The diffusivity map associated with HAD Anxiety scores (Figure 1A-C) shows a prominent lower intensity along the corpus callosum, indicating that greater anxiety was linked to higher diffusivity. This hypothesis has some support from DTI studies examining PSA (Ferro et al., 2016) as well as anxiety disorders (Saar-Ashkenazy et al., 2023; Lu et al., 2018; Kartashov et al., 2020). The diffusivity map negatively associated with CES-D scores (Figure 1D-F) shows high intensity in the posterior right hemisphere, indicating that higher PSD scores were linked with the frontal lobe and lesions in the left hemisphere. While there is some consensus in the literature on frontal lobe lesions contributing to psychiatric mood impairments (Ríos et al., 2025, Siddiqi et al., 2023), the role of laterality on PSD is controversial. Robinson et al. (2024) have repeatedly found patients with left hemisphere strokes to have an elevated risk of PSD. However, other meta-analyses have reported no association at all, or a weak association with the right hemisphere instead (Douven et al., 2017; Wei et al., 2015). Nevertheless, it would be prudent not to compare the importance of each hemisphere but observe how imbalances between the two impact mood; studies using graph theory, a quantitative network-based approach, have demonstrated the underlying role of imbalance across regions or hemispheres for several psychiatric disorders (Chang et al., 2021; Jiang et al., 2019; Bouttier et al., 2022). The advantage of our pipeline is

that it provides information on latent properties of the entire brain in a single step that may typically require several different imaging sequences to acquire. It would be a valuable improvement if the brain components identified through our approach could be characterized to provide complementary results to graph theory analyses.

However, the neurobiological interpretability of the emotional brain components is inherently ambiguous. They may potentially reflect composite or emergent properties of tissue microstructure as opposed to well-defined anatomical or functional substrates. Moreover, the diffusivity maps used to represent these neural components are not always readily interpretable, as secondary PCA components that explain limited variance typically fail to exhibit distinct patterns. This limitation represents a trade-off due to the global nature of our methodology, which should be addressed through further investigation.

We have only tested the pipeline using three-directional diffusion sequences. Although we verified that apparent diffusion coefficient (ADC) maps - which are often preferred for cross-study comparability due to their quantitative scaling - could be alternatively used, ADC values are dependent on model fitting assumptions and scanner-specific preprocessing steps (Malyarenko et al., 2014). Consequently, the generalizability of spatial patterns we obtained may be reduced. A further step would be to evaluate how white matter disruptions can be incorporated as a covariate, either from fluid-attenuated inversion recovery (FLAIR) images or from DTI images in the form of microstructural properties, to improve the pipeline's neurobiological justification. Considering that the pipeline relies on diffusion intensities and not specifically on the presence of strokes, it may be worth examining whether its predictability can be replicated in DWI images of other neurological disorders.

Beyond neuroimaging aspects, certain limitations of our work should be noted. Our results also depend on the standardized clinical scores of three French hospital-based cohorts with mild-to-moderate stroke patients and must therefore be validated in larger, culturally different populations. Additionally, we only utilized two self-reported mood evaluations, among which we did not have data for the specific dimensions of the CES-D in one of the cohorts. It will be important to test the pipeline with observer-rated scales of anxiety and depression as well as with other multidimensional neuropsychological evaluations.

CONCLUSION

We designed a pipeline to predict perceived levels of anxiety and depression symptomatology six months following stroke, relying only on routine clinical MRI images. It proved to be a viable technique in cases where a dedicated lesion disconnectome approach

could not be used. The simplicity of its design and underlying rationale act as a new potential avenue into network-level analyses. With further development, it may be utilized to establish how diffusion characteristics affect post-stroke neuropsychiatric symptoms.

REFERENCES

Altman, N. S. (1992). An Introduction to Kernel and Nearest-Neighbor Nonparametric Regression. The American Statistician, 46(3), 175–185. https://doi.org/10.1080/00031305.1992.10475879

Avants, B. B., Tustison, N., & Song, G. (2009). Advanced normalization tools (ANTS). Insight j, 2(365), 1-35. https://doi.org/10.54294/uvnhin

Bickle, J. (2012). A brief history of neuroscience's actual influences on mind–brain reductionism. In S. Gozzano & C. S. Hill (Eds.), New Perspectives on Type Identity: The Mental and the Physical (pp. 88–110). chapter, Cambridge: Cambridge University Press. https://doi.org/10.1017/CBO9780511687068.005

Bolboacă, S. D. (2019). Medical diagnostic tests: a review of test anatomy, phases, and statistical treatment of data. Computational and mathematical methods in medicine, 2019(1), 1891569. https://doi.org/10.1155/2019/1891569

Bota, M., Sporns, O., & Swanson, L. W. (2015). Architecture of the cerebral cortical association connectome underlying cognition. Proceedings of the National Academy of Sciences, 112(16), E2093-E2101. https://doi.org/10.1073/pnas.1504394112

Bouttier, V., Duttagupta, S., Denève, S., & Jardri, R. (2022). Circular inference predicts nonuniform overactivation and dysconnectivity in brain-wide connectomes. Schizophrenia Research, 245, 59-67. https://doi.org/10.1016/j.schres.2020.12.045

Chang, M., Womer, F. Y., Gong, X., Chen, X., Tang, L., Feng, R., ... & Wang, F. (2021). Identifying and validating subtypes within major psychiatric disorders based on frontal–posterior functional imbalance via deep learning. Molecular psychiatry, 26(7), 2991-3002. https://doi.org/10.1038/s41380-020-00892-3

Cunningham, P., & Delany, S. J. (2021). K-nearest neighbour classifiers-a tutorial. ACM computing surveys (CSUR), 54(6), 1-25. https://doi.org/10.1145/3459665

Douven, E., Köhler, S., Rodriguez, M. M., Staals, J., Verhey, F. R., & Aalten, P. (2017). Imaging markers of post-stroke depression and apathy: a systematic review and meta-analysis. Neuropsychology review, 27(3), 202-219. https://doi.org/10.1007/s11065-017-9356-2

Duttagupta, S., Castano, L., Chanraud, S., Sibon, I., Berthoz, S. (2026) Identifying clinico-radiological determinants of post-stroke fatigue 3 months post-stroke in a French hospital-based cohort of non-severe stroke patients without psychiatric comorbidities. PLOS ONE 21(3): e0345376. https://doi.org/10.1371/journal.pone.0345376

Ferro, J. M., Caeiro, L., & Figueira, M. L. (2016). Neuropsychiatric sequelae of stroke. Nature reviews. Neurology, 12(5), 269–280. https://doi.org/10.1038/nrneurol.2016.46

Godefroy O, Leclercq C, Roussel M, Moroni C, Quaglino V, Beaunieux H, et al; GRECOG-VASC Neuropsychological Committee. French adaptation of the vascular cognitive impairment harmonization standards: the GRECOG-VASC study. Int J Stroke. 2012;7:362–363. https://doi.org/10.1111/j.1747-4949.2012.00794.x

Herbet, G., & Duffau, H. (2020). Revisiting the functional anatomy of the human brain: toward a meta-networking theory of cerebral functions. Physiological reviews, 100(3), 1181-1228. https://doi.org/10.1152/physrev.00033.2019

Isensee, F., Schell, M., Pflueger, I., Brugnara, G., Bonekamp, D., Neuberger, U., ... & Kickingereder, P. (2019). Automated brain extraction of multisequence MRI using artificial neural networks. Human brain mapping, 40(17), 4952-4964. https://doi.org/10.1002/hbm.24750

Jiang, X., Shen, Y., Yao, J., Zhang, L., Xu, L., Feng, R., ... & Wang, J. (2019). Connectome analysis of functional and structural hemispheric brain networks in major depressive disorder. Translational psychiatry, 9(1), 136. https://doi.org/10.1038/s41398-019-0467-9

Kartashov, S., Tetereva, A., & Martynova, O. (2020). Reproducible Correlations Of Corpus Callosum And Cingulum Generalized Fractional Anisotropy With Anxiety Ratings In Healthy Participants. bioRxiv, 2020-12. https://doi.org/10.1101/2020.12.08.404608

Knapp, P., Dunn-Roberts, A., Sahib, N., Cook, L., Astin, F., Kontou, E., & Thomas, S. A. (2020). Frequency of anxiety after stroke: an updated systematic review and meta-analysis of observational studies. International Journal of Stroke, 15(3), 244-255. https://doi.org/10.1177/1747493019896958

Lépine JP, Godchau M, Brun P, Lempérière T. Evaluation de l'anxiété et de la dépression chez des patients hospitalisés dans un service de médecine interne [Evaluation of anxiety and depression among patients hospitalized on an internal medicine service]. Ann Med Psychol (Paris). 1985;143(2):175-189.

Lim, J. S., Lee, J. J., & Woo, C. W. (2021). Post-stroke cognitive impairment: pathophysiological insights into brain disconnectome from advanced neuroimaging analysis techniques. Journal of Stroke, 23(3), 297-311. https://doi.org/10.5853/jos.2021.02376

Liu, F., Gong, L., Zhao, H., Li, Y. L., Yan, Z., & Mu, J. (2024). Validity of evaluation scales for post-stroke depression: a systematic review and meta-analysis. BMC neurology, 24(1), 286. https://doi.org/10.1186/s12883-024-03744-7

Liu, L., Xu, M., Marshall, I. J., Wolfe, C. D., Wang, Y., & O'Connell, M. D. (2023). Prevalence and natural history of depression after stroke: A systematic review and meta-analysis of observational studies. PLoS medicine, 20(3), e1004200. https://doi.org/10.1371/journal.pmed.1004200

Lovrić, M., Đuričić, T., Tran, H. T., Hussain, H., Lacić, E., Rasmussen, M. A., & Kern, R. (2021). Should we embed in chemistry? A comparison of unsupervised transfer learning with PCA, UMAP, and VAE on molecular fingerprints. Pharmaceuticals, 14(8), 758.https://doi.org/10.3390/ph14080758

Lu, M., Yang, C., Chu, T., & Wu, S. (2018). Cerebral white matter changes in young healthy individuals with high trait anxiety: a tract-based spatial statistics study. Frontiers in neurology, 9, 704. https://doi.org/10.3389/fneur.2018.00704

Malyarenko, D. I., Ross, B. D., & Chenevert, T. L. (2014). Analysis and correction of gradient nonlinearity bias in apparent diffusion coefficient measurements. Magnetic resonance in medicine, 71(3), 1312-1323. https://doi.org/10.1002/mrm.24773

Matsulevits, A., Coupé, P., Nguyen, H. D., Talozzi, L., Foulon, C., Nachev, P., ... & Thiebaut de Schotten, M. (2024). Deep learning disconnectomes to accelerate and improve long-term predictions for post-stroke symptoms. Brain Communications, 6(5), fcae338. https://doi.org/10.1093/braincomms/fcae338

Matsulevits, A., Alvez, P., Atzori, M., Beyh, A., Corbetta, M., Del Pup, F., ... & de Schotten, M. T. (2025). A global effort to benchmark predictive models and reveal mechanistic diversity in long-term stroke outcomes. bioRxiv, 2024-10. https://doi.org/10.1101/2024.10.17.618691

Medeiros, G. C., Roy, D., Kontos, N., & Beach, S. R. (2020). Post-stroke depression: A 2020 updated review. General hospital psychiatry, 66, 70–80. https://doi.org/10.1016/j.genhosppsych.2020.06.011

Moore, M. J., Demeyere, N., Rorden, C., & Mattingley, J. B. (2024). Lesion mapping in neuropsychological research: A practical and conceptual guide. Cortex; a journal devoted to the study of the nervous system and behavior, 170, 38–52. https://doi.org/10.1016/j.cortex.2023.10.001

Morin, A. J., Moullec, G., Maiano, C., Layet, L., Just, J. L., & Ninot, G. (2011). Psychometric properties of the Center for Epidemiologic Studies Depression Scale (CES-D) in French clinical and nonclinical adults. Revue d'epidemiologie et de sante publique, 59(5), 327-340. https://doi.org/10.1016/j.respe.2011.03.061

Munsch F, Sagnier S, Asselineau J, Bigourdan A, Guttmann CR, Debruxelles S, Poli M, Renou P, Perez P, Dousset V, Sibon I. Stroke location is an independent predictor of cognitive outcome. Stroke. 2016 Jan;47(1):66-73. https://doi.org/10.1161/STROKEAHA.115.011242

Oakes, P., Loukas, M., Oskouian, R. J., & Tubbs, R. S. (2017). The neuroanatomy of depression: A review. Clinical Anatomy, 30(1), 44-49. https://doi.org/10.1002/ca.22781

Park, H. J., & Friston, K. (2013). Structural and functional brain networks: from connections to cognition. Science, 342(6158), 1238411. http://doi.org/10.1126/science.1238411

Parker, D. (2023). Assumptions of twentieth-century neuroscience: reductionist and computational paradigms. Interdisciplinary Science Reviews, 48(2), 217-234. https://doi.org/10.1080/03080188.2022.2149736

Pedregosa, F., Varoquaux, G., Gramfort, A., Michel, V., Thirion, B., Grisel, O., ... & Dubourg, V. (2011). Scikit-learn: Machine learning in Python: the Journal of machine Learning research, v. 12.

Pessoa L. (2023). How many brain regions are needed to elucidate the neural bases of fear and anxiety?. Neuroscience and biobehavioral reviews, 146, 105039. https://doi.org/10.1016/j.neubiorev.2023.105039

Ríos, A. S., Temuulen, U., Khalil, A. A., Villringer, K., Ali, H. F., Akdeniz, A., ... & Kufner, A. (2025). Lesion-Network Mapping of Poststroke Depressive Symptoms: Evidence From Two Prospective Ischemic Stroke Cohorts. Stroke, 56(9), 2527-2539. https://doi.org/10.1161/STROKEAHA.125.051858

Robinson, R. G., Jorge, R. E., & Starkstein, S. E. (2024). Poststroke Depression: An Update. The Journal of neuropsychiatry and clinical neurosciences, 36(1), 22–35. https://doi.org/10.1176/appi.neuropsych.21090231

Saar-Ashkenazy, R., Guez, J., Jacob, Y., Veksler, R., Cohen, J. E., Shelef, I., ... & Benifla, M. (2023). White-matter correlates of anxiety: The contribution of the corpus-callosum to the study of anxiety and stress-related disorders. International Journal of Methods in Psychiatric Research, 32(4), e1955. https://doi.org/10.1002/mpr.1955

Sagnier, S., Munsch, F., Bigourdan, A., Debruxelles, S., Poli, M., Renou, P., ... & Sibon, I. (2019). The influence of stroke location on cognitive and mood impairment. A voxel-based lesion-symptom mapping study. Journal of Stroke and Cerebrovascular Diseases, 28(5), 1236-1242. https://doi.org/10.1016/j.jstrokecerebrovasdis.2019.01.010

Sagnier, S., Catheline, G., Dilharreguy, B., Linck, P. A., Coupé, P., Munsch, F., ... & Sibon, I. (2020). Normal-appearing white matter integrity is a predictor of outcome after ischemic stroke. Stroke, 51(2), 449-456. https://doi.org/10.1161/STROKEAHA.119.026886

Siddiqi, S. H., Kletenik, I., Anderson, M. C., Cavallari, M., Chitnis, T., Glanz, B. I., ... & Fox, M. D. (2023). Lesion network localization of depression in multiple sclerosis. Nature Mental Health, 1(1), 36-44. https://doi.org/10.1038/s44220-022-00002-y

Talozzi, L., Forkel, S. J., Pacella, V., Nozais, V., Allart, E., Piscicelli, C., ... & Thiebaut de Schotten, M. (2023). Latent disconnectome prediction of long-term cognitive-behavioural symptoms in stroke. Brain, 146(5), 1963-1978. https://doi.org/10.1093/brain/awad013

Thiebaut de Schotten, M., Dell'Acqua, F., Ratiu, P., Leslie, A., Howells, H., Cabanis, E., ... & Catani, M. (2015). From Phineas Gage and Monsieur Leborgne to HM: revisiting disconnection syndromes. Cerebral cortex, 25(12), 4812-4827. https://doi.org/10.1093/cercor/bhv173

Thiebaut de Schotten, M., & Forkel, S. J. (2022). The emergent properties of the connected brain. Science, 378(6619), 505-510. https://doi.org/10.1126/science.abq2591

Van Essen, D. C., Ugurbil, K., Auerbach, E., Barch, D., Behrens, T. E., Bucholz, R., ... & WU-Minn HCP Consortium. (2012). The Human Connectome Project: a data acquisition perspective. Neuroimage, 62(4), 2222-2231. https://doi.org/10.1016/j.neuroimage.2012.02.018

Wei, N., Yong, W., Li, X., Zhou, Y., Deng, M., Zhu, H., & Jin, H. (2015). Post-stroke depression and lesion location: a systematic review. Journal of neurology, 262(1), 81-90. https://doi.org/10.1007/s00415-014-7534-1

SUPPLEMENTARY MATERIAL CAPTIONS

Supplementary 1: Intercohort comparisons of clinical and demographic characteristics
Supplementary 2: Univariate analysis between clinical variables and 6-month scores
Supplementary 3: Clinical model parameters
Supplementary 4: Technical limitations of disconnectome models
Supplementary 5: Results from the pipeline using ADC maps instead of DWI images

STATEMENTS & DECLARATIONS

Consent to participate and publish

Informed written consent was obtained from all individual participants in the study.

Funding

The cohort studies were supported by public grants from the French Ministry of Health (BBS: DGOS/PF4/2011/420; MOTIV-POSDEP: PHRC-17-0377; GRECOGVasc: DGOS R1/2013/144), the Translational Research and Advanced Imaging Laboratory (BBS: ANR-10-LABX-57) and the French National Research Agency (ANR) within the context of the France 2030 Program (MOTIV-POSDEP: ANR-23-IAHU-0001). S.D. is a PhD student funded by the Neurocampus International Graduate Program managed by the French National Agency program (ANR-17-EURE-0028).

Competing interests

The authors have no relevant financial or non-financial interests to disclose.

Ethics approval

All cohort studies were conducted in accordance with the Declaration of Helsinki. The Institutional Review Boards and local ethics committee approved the study protocols: BBS and MOTIV-POSDEP: Comité de Protection des Personnes Sud-Ouest et Outre Mer III; GRECOGVasc: Comité de Protection des Personnes d'Ile-de-France II.

Code availability

The code for designing the complete pipeline is in the online repository https://github.com/SuhritD/pca-prediction-pipeline

Supplementary Files

This is a list of supplementary files associated with this preprint. Click to download.

- Supplementary1.docx
- Supplementary2.docx
- Supplementary3.docx
- Supplementary4.docx
- Supplementary5.docx